Holocene sea surface conditions in the western North Atlantic: Spatial and temporal heterogeneities

Sandrine Solignac,[1] Jacques Giraudeau,[2] and Anne de Vernal[1]

Received 11 May 2005; revised 21 November 2005; accepted 11 January 2006; published 19 April 2006.

[1] Holocene records of sea surface conditions in the western Nordic seas were obtained from quantitative reconstructions based on dinoflagellate cyst assemblages. Two sediment cores from the east Greenland and the north Iceland shelves provide a detailed account of the long- and short-term dynamics of the opposing flows of Arctic versus Atlantic waters. Both marker species and quantitative reconstructions depict an overall trend toward warmer winter temperatures, saltier surface waters, and decreased sea ice extent. The latter is supported by a close relationship between relative abundances of an Atlantic dinocyst species, *Nematosphaeropsis labyrinthus*, and ice-rafted debris (IRD) records. We propose that the late Holocene increased IRD delivery in the Denmark Strait region was primarily induced by a combination of less extensive sea ice cover under increased Atlantic water inflow and sustained iceberg calving tied to the readvance of the Greenland ice sheet. Our records thus suggest diminishing polar water supplies throughout the Holocene, although the timing of regime changes differs between the western and eastern sides of the Denmark Strait. Finally, comparison of our records with a core from southern Greenland points to very heterogeneous sea surface conditions in the western North Atlantic, which could be explained by the decoupled dynamics of the two Irminger Current branches. Similarities between the southern Greenland marine record and a continental record nearby suggest a close coupling with atmospheric processes, reminiscent of a North Atlantic Oscillation–like climate pattern.

Citation: Solignac, S., J. Giraudeau, and A. de Vernal (2006), Holocene sea surface conditions in the western North Atlantic: Spatial and temporal heterogeneities, *Paleoceanography*, *21*, PA2004, doi:10.1029/2005PA001175.

1. Introduction

[2] Holocene climate variability has been the focus of numerous studies in the recent years. There is a general consensus on a climate transition in the mid-Holocene [e.g., *Steig*, 1999], generally attributed to insolation changes [e.g., *Alley et al.*, 1999; *Marchal et al.*, 2002]. In addition, growing evidence suggest that higher-frequency oscillations are superimposed on this long-term trend, in atmospheric [*O'Brien et al.*, 1995], continental [*Campbell et al.*, 1998], sea surface [*Bond et al.*, 1997], as well as deep-sea [*Bianchi and McCave*, 1999] records. However, many inconsistencies are observed between the records, with respect for instance to the timing of these oscillations, their periodicities, their cause and their spatial extent [e.g., *Solignac et al.*, 2004].

[3] The spatial extent of climate fluctuations, either on a long or short term, is an important factor to assess as it can shed light on climate mechanisms (e.g., seesaw patterns as in the North Atlantic Oscillation versus global temperature trends). Here we aim at understanding sea surface changes throughout the Holocene in different domains of the Nordic seas, which are characterized by pronounced temperature and salinity gradients due to the presence of very contrasting water masses, as well as by a strong sensitivity to climate changes related to their high-latitude setting. In particular, the Denmark Strait is a central region when addressing the sea surface variability of the Nordic seas as it extends over very different interacting environments, characterized by Arctic water outflow to the west and by the influence of warm and saline North Atlantic waters to the east. Recent paleoenvironmental studies have highlighted the sensitivity of this oceanic realm to subtle changes in climate variations and ocean processes throughout the last 10,000 years [*Andrews et al.*, 2002; *Jennings et al.*, 2002; *Knudsen et al.*, 2004; *Andresen et al.*, 2005]. Two study sites were thus chosen on each side of the Denmark Strait in order to document the recent history of Atlantic and Arctic sea surface and its influence on the heat and salt budget of the western North Atlantic.

[4] Sea surface parameters (temperature, salinity and sea ice extent) were reconstructed for the past 10,000 calibrated years on the basis of organic-walled dinoflagellate cyst (dinocyst) assemblages. Dinocysts are a sensitive proxy for sea surface conditions and allow the reconstruction of hydrographical parameters including temperature and salinity of the coldest and warmest months, salinity and sea ice cover extent [e.g., *de Vernal et al.*, 1994, 2005].

2. Oceanographic Setting

[5] The cold and relatively fresh East Greenland Current (EGC) flows south from the Arctic Ocean in a narrow band

[1]Centre de Recherche en Géochimie Isotopique et Géochronologie, Université du Québec à Montréal, Montreal, Quebec, Canada.
[2]Environnements et Paléoenvironnements Océaniques, UMR CNRS 5805, Université Bordeaux 1, Talence, France.

0883-8305/06/2005PA001175

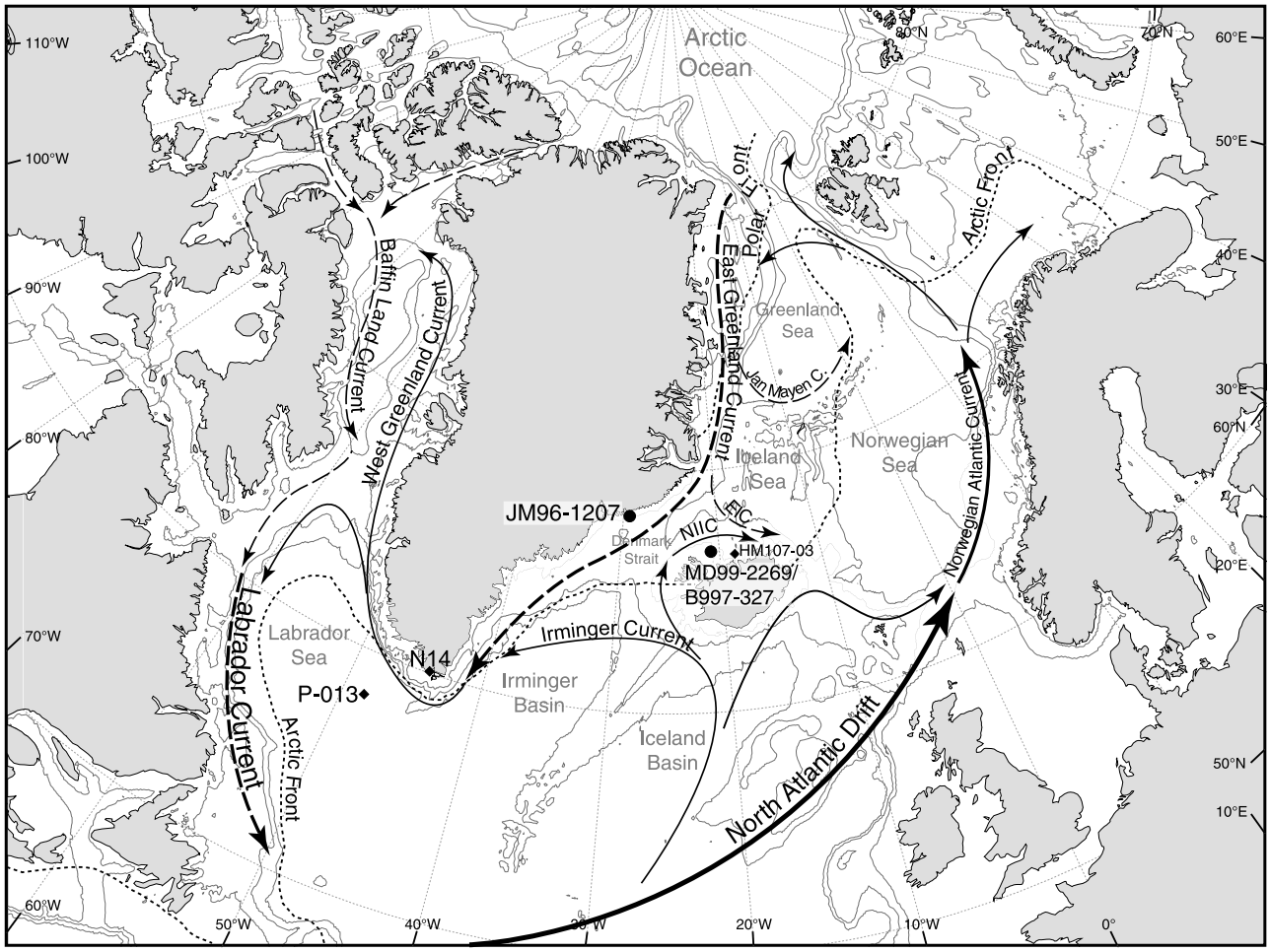

Figure 1. Location of the study cores MD99-2269, B997-327, and JM96-1207, and trajectories of the main ocean surface currents. Dashed arrows represent cold currents and solid arrows represent warm currents. The dotted lines illustrate the Arctic and Polar fronts, that is, the maximum sea ice extension in winter and summer, respectively, as defined from the 1953–2003 data set provided by the *National Snow and Ice Data Center* (*NSIDC*) [2003] and the sea ice atlas prepared by the *Naval Oceanography Command Detachment* [1986]. Locations of cores P-013 and HM107-03 and Lake N14 [*Andresen et al.*, 2004], to which we refer in the text, are indicated. Isobaths indicate water depths of 2000, 1000, and 200 m.

along the Greenland coast. Part of it splits and feeds the Jan Mayen Current (JMC) in the Greenland Sea, as well as the East Iceland Current (EIC) in the Iceland Sea. The ice-free EIC usually carries Arctic water to the northern Iceland shelf; however, the EIC can acquire a true polar character, in connection with a strengthened EGC and northerly wind conditions [*Malmberg*, 1985; *Ólafsson*, 1999].

[6] The Irminger Current (IC) branches from the warm and saline North Atlantic Drift. Part of it flows westward into the Irminger basin, whereas the other branch circulates anticyclonically around Iceland (Figure 1) [*Johannessen*, 1986]. Hence west and north of Iceland, close to the coast, warmer water is brought by the slightly modified northern branch of the IC, the North Iceland Irminger Current (NIIC). The environment of the northern Icelandic shelf is thus highly variable and primarily controlled by the balance between the relative strength of the Atlantic NIIC and the Arctic EIC [*Malmberg and Jónsson*, 1997].

[7] The presence of hydrographically contrasting water masses in the Nordic seas gives rise to the formation of two major oceanic fronts (Figure 1). The Polar Front corresponds with the maximum extent of summer sea ice and marks the boundary between the purely polar waters carried by the EGC and the Arctic waters of the Greenland and Iceland seas, which are saltier and warmer because of the influence of Atlantic waters brought by the Irminger and Norwegian Atlantic currents [*Johannessen*, 1986] (Figure 1). The Polar Front thus closely follows the eastern Greenland coast. The Arctic Front coincides with the maximum winter sea ice extent and separates the Arctic waters from the Atlantic waters flowing north along the Norwegian coast as the Norwegian Atlantic Current (NAC, Figure 1).

[8] The surface currents described above have obvious consequences on the sea ice formation and distribution. On the northeastern margin of Greenland, sea ice cover in the fjords and on the shelf lasts several months a year, in the

form of either landfast ice or drifting polar pack ice [*Andrews et al.*, 2002; *Jennings et al.*, 2002]. In summer and fall, higher solar radiation allows runoff from the continent and melts the sea ice and icebergs, hence reducing the sea surface salinity [*Andrews et al.*, 2002].

[9] Generally, no sea ice is observed on the Iceland shelf, except in a few bays. Sea ice formation can nevertheless occur on the northern shelf in winter when surface salinity decreases. Severe ice conditions can also develop there in times of high export of sea ice from the Arctic Ocean and east Greenland shelf, when influence of the Arctic EIC dominates over that of the IC waters [*Hopkins*, 1991; *Andrews et al.*, 2001b, 2002]. The Great Salinity Anomaly (GSA) in the 1960s is a good example of such a phenomenon. Enhanced northerly winds induced by a strengthened Greenland High increased the strength of the EGC, as well as the export of sea ice from the Arctic Ocean through the Fram Strait, resulting in a higher contribution of the polar water to the EIC. The EIC salinity then decreased to 34.7, allowing stratification and sea ice formation on the north Icelandic shelf [*Belkin et al.*, 1998; *Visbeck et al.*, 2003].

3. Materials and Methods

[10] Core JM96-1207/1-GC (68°06′N, 29°21′W; water depth 404 m) was collected in the Nansen trough on the inner east Greenland shelf in 1996 aboard the Norwegian R/V *Jan Mayen* [*Jennings et al.*, 2002]. The site lies in an area influenced by the EGC and is therefore characterized by low temperatures and salinity of $\leq$0°C, and $\leq$34.5 respectively. Sea ice cover lasts over 6 months a year and icebergs from the Greenland ice sheet and glaciers can be carried to the south by the ECG [*Andrews et al.*, 1997; *Jennings et al.*, 2002].

[11] Core B997-327 (66°38′N, 20°52′W; water depth 373 m) was retrieved on the northern Iceland continental shelf during the summer 1997 cruise of R/V *Bjarni Saemundsson* [*Helgadóttir*, 1997]. MD99-2269 (66°37′N, 20°51′W, water depth 365 m) was raised at the same site during the IMAGES V cruise of R/V *Marion Dufresne* in 1999. The northern Iceland shelf is under the influence of the warm and ice free NIIC (7°–12°C, 35). However, the NIIC influence can diminish in favor of polar waters ($\leq$0°C) brought by the EIC, in which case severe ice conditions establish [*Andrews et al.*, 2002].

[12] Cores will be referred to in the text as 1207, 327 and 2269.

3.1. Chronologies

[13] The stratigraphic framework for core 1207 has been described by *Jennings et al.* [2002]. It is based on 7 AMS ^{14}C dates, three of which having been measured on a nearby core (JM96-1206, 68°06′N, 29°26′W; water depth 402 m) correlated to the 1207 with the use of their respective volume magnetic susceptibility profiles. A marine reservoir correction of 550 years was applied to all dates, following the work of *Hjort* [1973] on the east Greenland shelf. Two linear equations make up the age model, reflecting the sedimentation rate change at the transition from the Holocene marine mud to the Last Glacial glaciomarine pebbly mud [*Jennings et al.*, 2002] (Figure 2). The sedimentation rate throughout the Holocene is constant at 20 cm kyr^{-1}. The last ~0.34 kyr are missing from the sedimentary record.

[14] Chronology of core 327 is based on 4 AMS ^{14}C dates calibrated after a correction for a standard marine reservoir of 400 years as reported in previous works [*Andrews et al.*, 2001a; *Castañeda et al.*, 2004] (Figure 2). The age model developed here is given by a second-order polynomial equation: age (cal yrs BP) = $0.0412x^2 + 1.8997x + 385.71$ ($R^2 = 0.9996$), where x is the depth expressed in cm. Sedimentation rates range from ~550 cm kyr^{-1} at the very top of the core to ~37 cm kyr^{-1} at the base. The 3 m-long record of core 327 spans only the late Holocene (<4.8 ka) and lacks the last 0.38 kyr.

[15] Despite its proximity to core 327, core 2269 displays on average a higher sedimentation rate. The 11 calibrated AMS ^{14}C dates (400-year reservoir age correction), along with the Saksunarvatn tephra at 10.18 calibrated ka BP, indicate that sediment accumulated at a constant rate of ~200 cm kyr^{-1} during the entire Holocene [*Andrews et al.*, 2003; *Giraudeau et al.*, 2004] (Figure 2). The present study investigated the bottom 14 meters of core 2269, spanning 3.2 to 10.0 ka. A composite 2269/327 record was constructed using the stratigraphic frameworks obtained on both cores to analyze the Holocene time interval.

3.2. Dinocysts

[16] On core 1207, 1 cm-thick sediment slices were subsampled every 2 cm for the interval corresponding to the last 10,000 calibrated years. Core 2269 was subsampled every 5 or 10 cm, and core 327, every ~5 cm on the entire record. Temporal resolution of analyses is thus relatively high, ranging from ~135 years in the lowest sedimentation rate interval in core 327 to ~100 years in core 1207 and ~25–50 years in core 2269. This allows the investigation of millennial- to submillennial-scale sea surface circulation changes.

[17] Samples from the entire 1207 and 327 records, as well as samples spanning 10.0 to 3.2 ka from core 2269, were treated following standard techniques described by *de Vernal et al.* [1999] in order to recover dinocysts. On average, 300 dinocysts were counted and identified for each sample, following the taxonomic nomenclature of *Rochon et al.* [1999] and *Head et al.* [2001]. Heterotrophic brown cysts such as *Brigantedinium* spp., *Quinquecuspis* spp. or *Lejeunecysta* spp. are often hard to distinguish one from another when not properly oriented on the slide. Thus, when unidentifiable, these cysts were grouped in the Protoperidinioid category. Concentrations were calculated using the marker grain method [*Matthews*, 1969].

3.3. Sea Surface Condition Reconstructions

[18] Dinocysts, at least the autotrophic ones, thrive in the photic zone along with coccolithophores and diatoms in order to achieve photosynthesis. It has been shown that the distribution of the different dinocyst assemblages in the Nordic seas is closely related to water masses [*Matthiessen*, 1995], which make them good tracers of past sea surface conditions [*de Vernal et al.*, 1994, 2001].

[19] The best analogue technique of the PPPbase software [cf. *Guiot and Goeury*, 1996] was used for quantitative reconstructions of sea surface condition based on dinocyst

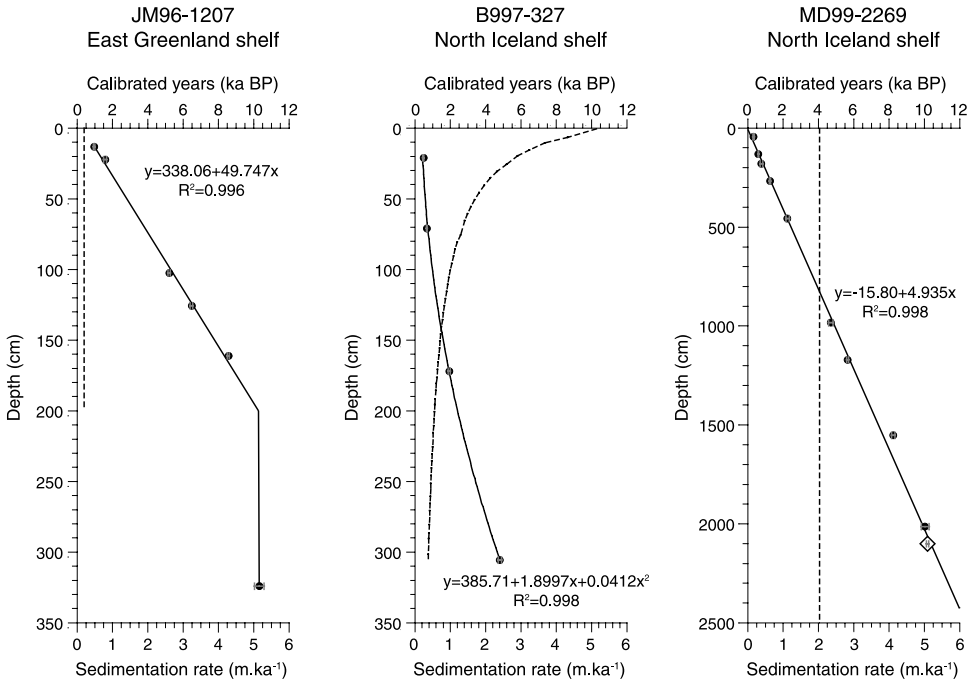

Figure 2. Age models of cores JM96-1207, B997-327, and MD99-2269. Dots represent ^{14}C dates. The diamond in core MD99-2269 corresponds to a tephra marker at 10.18 ka [*Giraudeau et al.*, 2004]. One of the ^{14}C dates of core MD99-2269 is absent from the graph as it is older than 12 calibrated ka. It was nevertheless taken into account in the regression calculations. Interpolated ages are indicated by black curves. Sedimentation rates are indicated by dashed curves. Note that a different depth scale was used for core MD99-2269.

assemblages. It allows the reconstruction of sea surface temperatures (SST) and sea surface salinities (SSS) in February and August, as well as sea ice cover extent, on the basis of the similarity between modern and fossil dinocyst spectra. Logarithm transformation of the relative abundances (per mil) of taxa is made to increase the weight of the secondary taxa, which often have more specific ecological affinities than ubiquitous dominant taxa, and therefore to better discriminate assemblages in relation to environmental parameters [*de Vernal et al.*, 2001, 2005]. The dinocyst database used here comprises 940 reference sites from the North Atlantic, North Pacific and Arctic oceans and their adjacent seas [*de Vernal et al.*, 2005]. Hydrographical data at 0 m of water depth (SSTs and SSSs, in February and August) for each of these reference sites were compiled from the 2001 World Ocean Atlas [*National Oceanographic Data Center* (*NODC*), 2001], which gathers instrumental measurements from 1900 to 2001. The extent (in months yr^{-1}) of sea ice cover with concentration greater than 50% was determined after the 1953–2003 data set of the *National Snow and Ice Data Center* [2003]. These two databases have the advantage of spanning 100 and 50 years, respectively. Hydrographical parameters assigned to each reference site are therefore averaged over a longer time period, which is more suited for surface sediments that might integrate several decades. The same sources were used to assess modern values of sea surface parameters at the two sites. Sea surface condition reconstructions were then made for the three records.

[20] Details on the approach used for quantitative reconstruction as well as the degree of accuracy of these reconstructions are thoroughly documented by *de Vernal et al.* [2005]. This method was proved particularly effective for reconstructing harsh environments such as those that characterized the northern Atlantic during the last glacial maximum. The accuracy of the method falls within the range of the modern hydrographical parameters variability and is better in more stable, open ocean environments [*de Vernal et al.*, 2005]. It shows a larger spread of estimated versus measured values in shallow and ice marginal areas such as those considered in the present study, which is explained by the high variability of sea surface conditions at annual, decadal or centennial timescales, and by the lack of accuracy of instrumental data in these specific settings [*Mudie and Rochon*, 2001]. In such cases, quantitative reconstructions are somewhat less reliable than in ice-free or open-ocean environments and should be interpreted with caution. A qualitative examination of the paleoenvironmental information given by the species assemblages is essential to validate the temporal trends of the quantitative reconstructions.

4. Results

4.1. Dinocyst Records

[21] The very different environments in which the cores were collected are reflected in the total dinocyst concentrations. They are lower in the colder Greenland environ-

ment of core 1207 (generally a few thousand dinocysts g^{-1}, with rare peaks of the order of 10^4 dinocysts g^{-1},) than in the composite 2269/327, where much higher concentrations, of the order of 10^5 to 10^6 dinocysts g^{-1}, are reached, peaking between 4.5 and 3.2 ka (Figure 3a). The general pattern of increasing concentrations from Greenland to north Iceland is in agreement with previous studies of dinocyst populations in surface sediment samples [*Matthiessen et al.*, 2001; *Marret et al.*, 2004]. In particular, the high total dinocyst concentrations recorded at site 2269/327 past 4.5 ka are of the order of those presently recorded off northern Iceland in the vicinity of the Arctic front [*Marret et al.*, 2004], and might depict the setting up of this highly productive frontal boundary which separates the Arctic waters from the Atlantic waters carried by the NIIC around western Iceland.

[22] Despite differences in hydrographical context and associated overall dinoflagellate production, both the east Greenland and the north Iceland shelves support an almost equally diverse (in terms of number of species) dinocyst population throughout the Holocene. However, the species assemblages are significantly different between the two sites, and changes in their composition are more pronounced at the east Greenland margin site.

[23] In core 2269/327, variations in the assemblages are mostly driven by changes in the relative abundances of *Operculodinium centrocarpum*, cysts of *Pentapharsodinium dalei*, and *Nematosphaeropsis labyrinthus*, followed by *Spiniferites ramosus* and *Spiniferites elongatus*, which altogether often account for more than 80% of the total spectra (Figure 3a). The overwhelming dominance in the lower Holocene of cysts of the ubiquitous polar to subpolar taxa *P. dalei*, with sustained occurrences of heterotrophic taxa such as *Brigantedinium* spp. and Protoperidinioids, are indicative of harsher conditions characterized by large seasonal differences in the physicochemical status of the surface waters and extensive sea ice cover as encountered in sheltered coastal waters of polar and Arctic domains [*de Vernal et al.*, 2001]. Heterotrophic taxa can indeed be seen as an indication of sea ice cover; while the growth of autotrophic taxa is inhibited because of a poor penetration of light, heterotrophs, which depend on food availability such as sea ice diatoms, can develop [*Matthiessen*, 1995]. Two transitions are worth noticing. At ~6.2 ka, percentages of *S. elongatus* and *Bitectatodinium tepikiense* increase to the expense of *S. ramosus. B. tepikiense* shows affinities for stratified waters with large seasonal temperature amplitudes and reduced sea ice cover [*Rochon et al.*, 1999], and therefore suggests the setting up of a highly dynamical frontal system. At ~4.9 ka, *O. centrocarpum* increases dramatically from ~10% to 50%. This increase is mainly offset by a drop in cysts of *P. dalei* and to a lesser extent in *S. elongatus.* The distribution of the cyst of *P. dalei* is often associated with strong seasonal temperature gradients and the presence of the Polar Front [*Marret et al.*, 2004], whereas both the global [*Rochon et al.*, 1999] and regional [*Boessenkool et al.*, 2001; *Marret et al.*, 2004] biogeographical dinocyst data sets point to the affinities of *O. centrocarpum* for cold-temperate, nutrient-rich surface waters such as the North Atlantic Drift. The replacement of cysts of *P. dalei* with *O. centrocarpum* at ~4.9 ka therefore suggests a decrease in polar waters supplies and the flooding of the north Icelandic shelf with modified Atlantic-sourced waters. This assumption is further strengthened by the gradual increase, from 3 ka onward, of the abundance of *N. labyrinthus*, a taxa which presently outcompetes other dinocysts species in surface sediment off southwestern Iceland bathed by the IC [*Marret et al.*, 2004]. The above-described change in dominance between the cysts of *P. dalei* and *O. centrocarpum*/*N. labyrinthus* is also apparent in the dinocyst record of core 1207 (Figure 3b), hereby suggesting that a change from polar to more Arctic/Atlantic conditions developed off both northern Iceland and eastern Greenland settings throughout the Holocene. However, both the timing and the amplitude of this regime change show some discrepancies on each side of the Denmark Strait.

[24] In core 1207, secondary taxa account for a greater part of the spectra variations. Since these subordinate taxa often thrive in environments with narrower variability in sea surface parameters, the fluctuations of their relative abundances carry more information on environmental changes than those of the dominant ubiquitous taxa. Hence we can infer from the assemblage changes in core 1207 that hydrographical parameters on the east Greenland shelf went through more pronounced fluctuations than on the northern Iceland shelf. The most obvious transition occurs at ~7.2 ka when heterotrophic taxa (*Islandinium minutum*, *Brigantedinium* spp., Protoperidinioids and *Selenopemphix quanta*), which make up 10 to 30% of the total assemblages in the early Holocene, disappear in favor of autotrophic taxa *S. elongatus* and *O. centrocarpum*. *I. minutum* occupies a restricted ecological niche in the North Atlantic with maximum abundance in surface sediments off central and northeastern Greenland and in the Greenland Sea, which are characterized by permanent to quasi-permanent sea ice cover [e.g., *de Vernal et al.*, 2001; *Head et al.*, 2001]. This drastic change in trophic characteristics of the assemblages suggest that the surface water regime went through a major reorganization at about 7.2 ka, from polar conditions with extensive sea ice cover to more open ocean-like conditions. A second reorganization is seen around 4.9 ka, when oceanic taxa *N. labyrinthus*, with maximum abundance in Atlantic/Irminger-influenced areas off Iceland [*Marret et al.*, 2004], and *I. pallidum*, which is highly successful in cold, fully marine environments [*de Vernal et al.*, 2001; *Matthiesen et al.*, 2005], appear. These transitions from neritic to more open-ocean assemblages bears to a certain extent some resemblance with the proximal and distal assemblages observed along the southeastern Greenland coast by *Boessenkool et al.* [2001]. The proximal assemblage is found on the inner shelf, where the influence of polar

Figure 3. Diagram of dinocyst assemblages (expressed in percentages) and total dinocyst concentrations (black curves on the right) for the past 10,000 calibrated years in cores (a) 2269/327 and (b) 1207. Note the different scales used for dominant and accompanying taxa. Dashed lines indicate transitions discussed in the text.

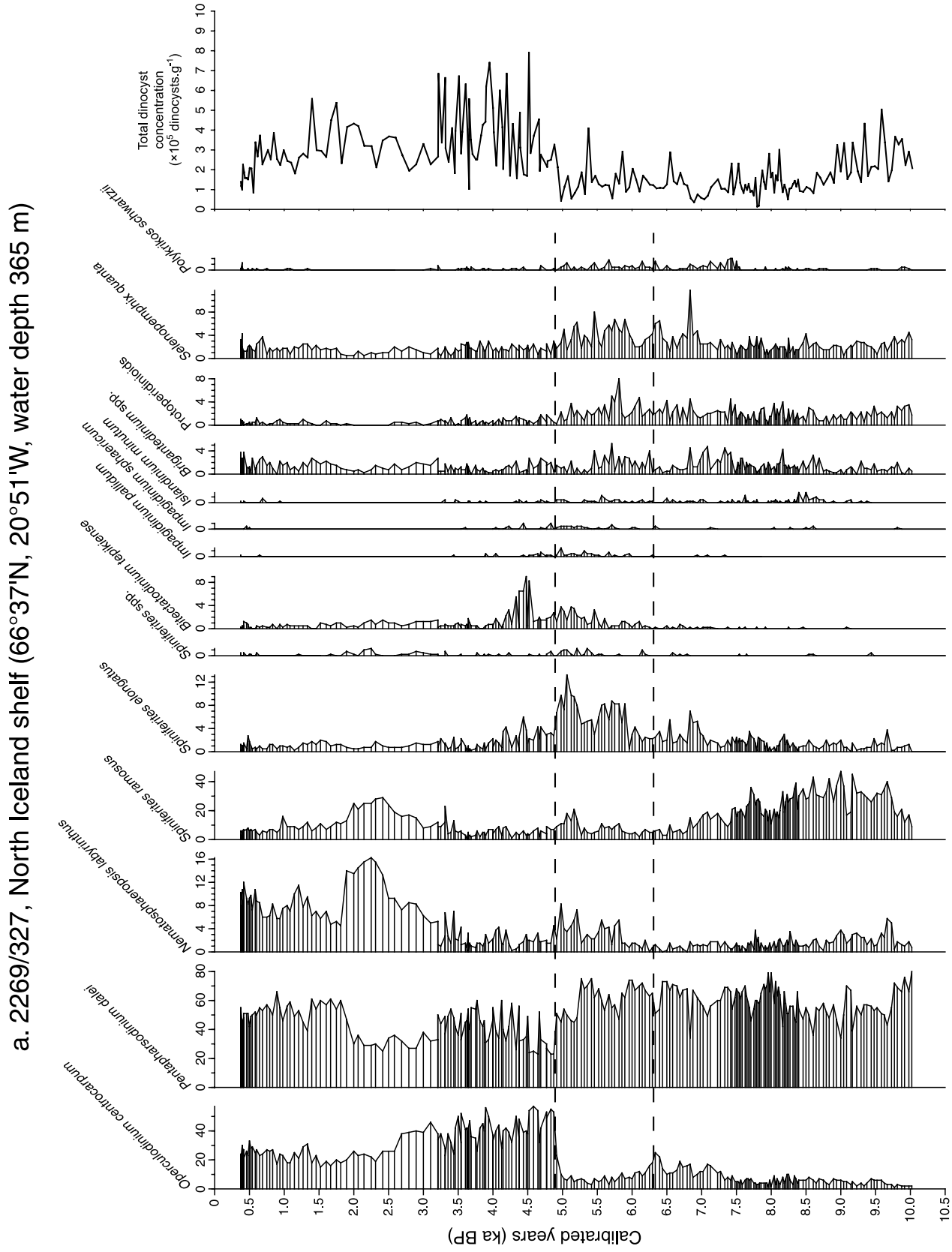
a. 2269/327, North Iceland shelf (66°37'N, 20°51'W, water depth 365 m)
Total dinocyst concentration (×10^5 dinocysts.g^-1)
Polykrikos schwartzii
Selenopemphix quanta
Protoperidinioids
Brigantedinium spp.
Islandinium minutum
Impagidinium sphaericum
Impagidinium pallidum
Bitectatodinium tepikiense
Spiniferites spp.
Spiniferites elongatus
Spiniferites ramosus
Nematosphaeropsis labyrinthus
Pentapharsodinium dalei
Operculodinium centrocarpum
Calibrated years (ka BP)

Figure 3

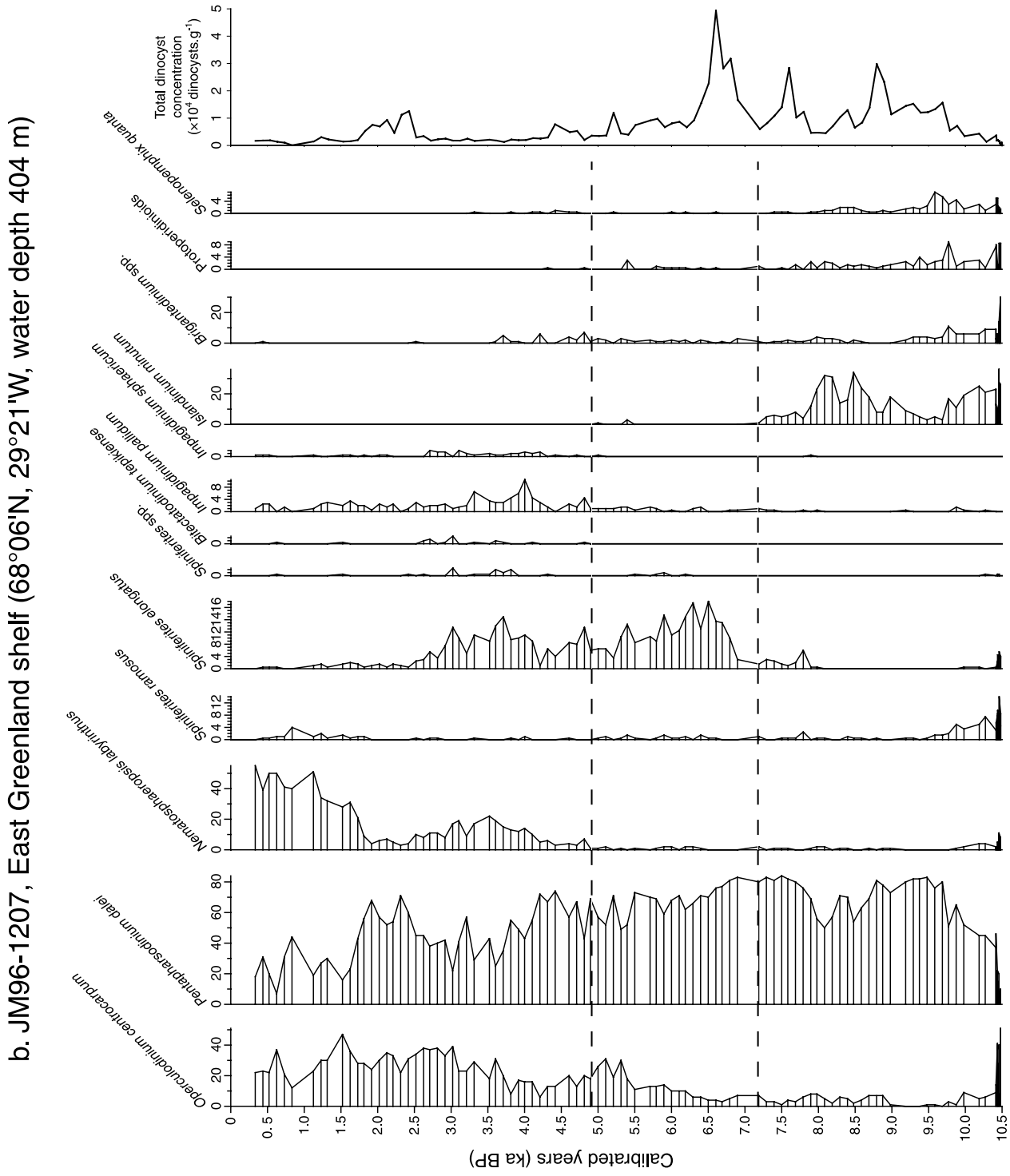

Figure 3. (continued)

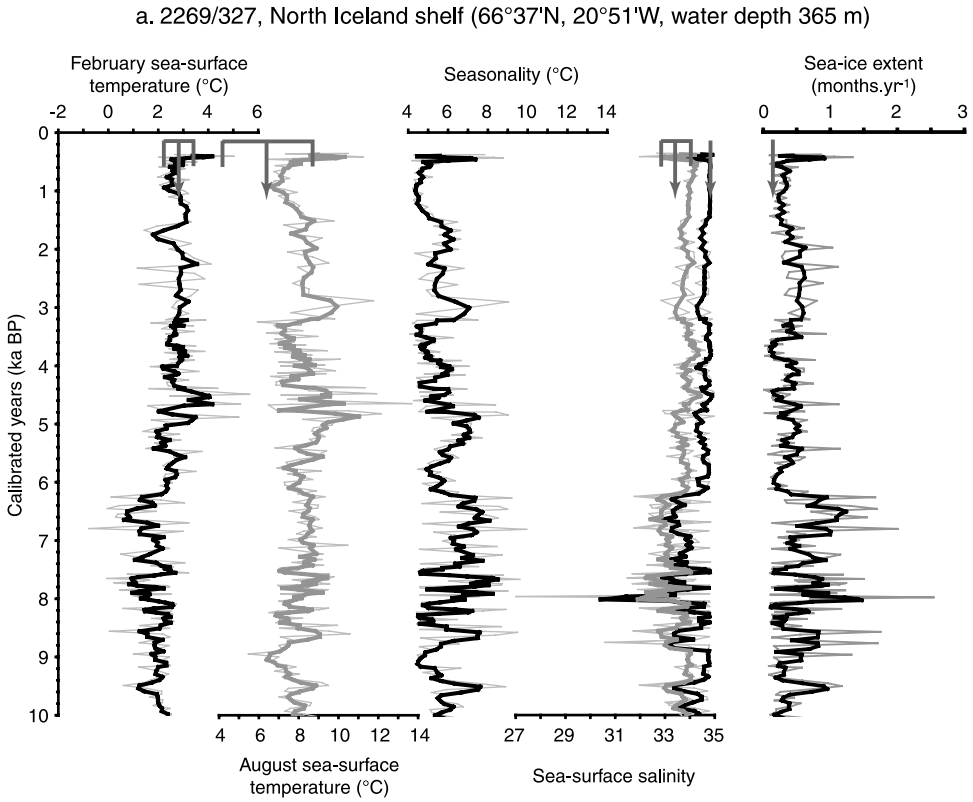

Figure 4. Reconstructions of sea surface conditions for the past 10,000 calibrated years for cores (a) 2269/327 and (b) 1207. Reconstructions are based on the five closest analogues following the procedure described by *de Vernal et al.* [2005]. Bold curves are smoothed records (three-point running mean). Black curves in temperature and salinity are February values, and gray curves are August values. Dark gray arrows represent modern values, compiled from the 1900–2001 record of the *National Oceanographic Data Center* (*NODC*) [2001] and the 1953–2003 ice record from *NSIDC* [2003]. The width of the base of the arrows shows the standard deviation of these modern instrumental measurements. No modern value was available for February SSSs in core 1207.

waters is the strongest, and comprises a significant proportion of heterotrophic taxa such as *I. minutum*. The distal assemblage, dominated by both *O. centrocarpum* and *N. labyrinthus*, characterizes the continental slope, where the influence of Atlantic waters is more pronounced. After ~4.9 ka, as recorded in core 2269/327, most of the variations in percentages of taxa concern the dominant species *O. centrocarpum*, cysts of *P. dalei* and *N. labyrinthus*, with a notable increase of the latter after 1.8 ka.

4.2. Sea Surface Reconstructions

[25] In spite of discrepancies in timing and amplitude of inferred hydrological regime changes, both the northern Iceland and eastern Greenland dinocyst records suggest that a shift from polar/Arctic to more Arctic/Atlantic conditions developed in the area of the Denmark Strait from the early to the late Holocene. The reconstructed sea surface parameters (Figure 4) are coherent with this inferred long-term pattern. They also emphasize the major differences in environmental settings between the two sites. February SSTs are constantly lower on the Greenland shelf than north of Iceland, with a difference of up to 3°C. In contrast, the gap between the 1207 and 2269/327 August SSTs records is much smaller; summer SSTs off Greenland can even be warmer than in the Iceland Sea, especially in the early Holocene. As a result, the temperature contrast (summer minus winter SSTs), hereafter referred to as seasonality, is generally higher, throughout the Holocene, off eastern Greenland, with the exception of a few short episodes. Apart from the very beginning of the Holocene, sea ice conditions are more severe on the Greenland shelf, lasting up to 6 months yr^{-1}, compared to the north Iceland shelf where there is no more than 1.5 months yr^{-1} of sea ice cover.

[26] On the northern Iceland shelf, reconstructions for the top of the core yield values close to the present (Figure 4a); reconstructed summer SSTs are slightly higher than today's values, part of this discrepancy being attributable to the fact that core 2269/327 lacks the last 0.38 ka, but they nevertheless fall within the range of modern variability (summer SSTs: 6.5°C ± 2.2, *NODC* [2001]). A comparison of our dinocyst-based reconstructions with diatom-based estimates for the last 5 calibrated kyr B.P. from a nearby coring site (HM107-03, same water depth, ca. 100 nm eastward [*Jiang et al.* [2002]) is shown in Figure 5. These summer SST reconstructions are based on a regional surface sediment

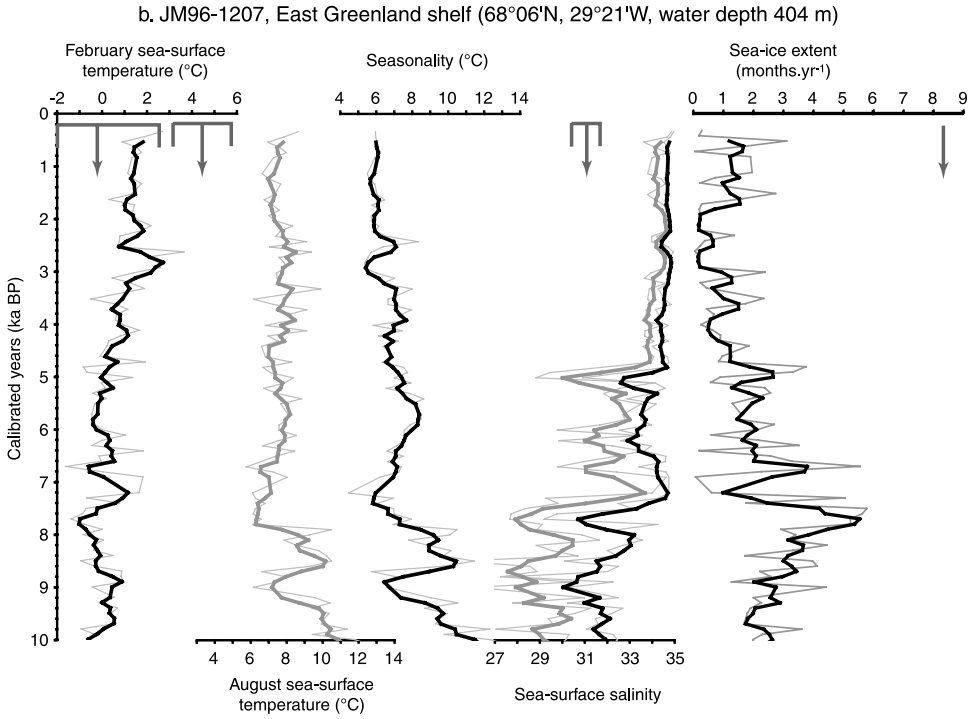

Figure 4. (continued)

diatom database that is highly representative of the range of environmental variables around Iceland [*Jiang et al.*, 2001]. With the exception of the last 1000 years, and despite an offset of ~1°C, both the trends and the range of variation of summer SSTs are strongly coherent between the two methods, supporting our dinocyst-based estimates from the northern Iceland shelf.

[27] In contrast, the gap between reconstructed hydrographical parameters and modern values seems to be much more important on the east Greenland shelf, with a difference of up to 5°C in summer SSTs, 4 in summer SSSs and 6 months in sea ice cover (Figure 4b). Both the quality of the instrumental data set and the peculiar hydrological context off eastern Greenland may, at least in part, explain these discrepancies: instrumental measurements in the region are very rare as shown by the absence of measured values for modern February SSSs in the *NODC* [2001] records. In addition, the location of site 1207 in the vicinity of the Polar Front, a hydrological boundary characterized by highly variable sea surface conditions on annual to centennial timescales [e.g., *Isemer and Hasse*, 1985], makes modern values on the basis of sparse measurements less reliable in this specific setting. Another possible source of divergence could be related to dinocyst production being lower during episodes of harsh conditions [*Matthiessen et al.*, 2001]; fossil assemblages would thus preferentially represent the most favorable years. Finally, a close examination of the dinocyst database reveals a lack of reference modern assemblages in the Denmark strait region. The closest analogues are therefore selected on the northern Iceland shelf and in the Norwegian Sea, which probably creates a bias toward warmer conditions. Still, we consider that the relative variations in the reconstructed parameters are valid, as they are supported by qualitative examination of the assemblages. Absolute values of reconstructions should therefore be taken with care and interpretations of the results should rather be based on the relative variations of sea surface conditions and on assemblage changes.

[28] Despite Greenland shelf being a colder environment than the Iceland shelf, long-term tendencies at both sites share some common features. Winter SSTs depict an increase from the mid-Holocene onward and sea ice seems to have been more extensive during the early Holocene. SSS shifts from low to more oceanic values in the mid-Holocene are also observed on both shelves. The long-term trends in seasonality show some similarities at both sites as well, as they are characterized by overall decreasing values throughout the Holocene (Figure 4). On a shorter timescale, however, there are discrepancies with respect to the timing and amplitude of sea surface condition oscillations.

[29] In both cores, very different environments from today characterize the early Holocene, as shown by the dinocyst assemblages and by the SSS and SST reconstructions. On the northern Iceland shelf, these reconstructions depict a distinct regime, with lower SSSs (~33.5), higher seasonality and a longer sea ice extent prior to 6.2 ka. Some marked high-amplitude oscillations are observed during this period, but no longer-term trend stands out (Figure 4a). Off east Greenland (Figure 3b), the early Holocene assemblage characterized by dominant heterotrophic and sea ice adapted taxa corresponds to very low SSSs (~30 and ~32 in summer and in winter, respectively), associated with generally higher summer SSTs (~9°C) than in the rest of the record. Throughout this interval ending at about 7.2 ka, summer SSTs strongly decrease, accordingly with an increase in the sea ice extent. Rapid, high-ampli-

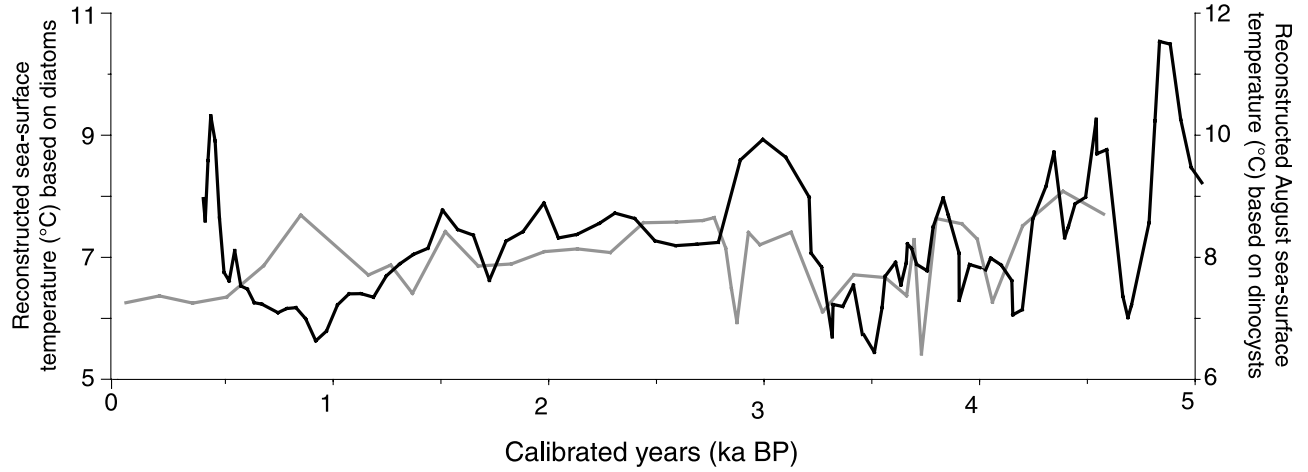

Figure 5. Comparison of diatom-based reconstructions of summer SSTs (core HM107-03, 66°30′N, 19°04′W [*Jiang et al.*, 2002], gray curve) with dinocyst-based August SSTs from core 2269/327 (black curve). Note that the scales were shifted in order to better illustrate the common variations.

tude fluctuations attest overall instable sea surface conditions (Figure 4b).

[30] In the mid-Holocene, major changes are recorded. After ~6.2 ka in core 2269/327, the regime change is expressed as a clear shift in most of the reconstructed parameters, toward higher values for SSTs and SSSs, and lower values for sea ice extent and seasonality. SSSs reach modern values and are much more stable than in the early Holocene. The variations in assemblages (Figure 3a) suggest recurrent millennial-scale, high-amplitude changes of modern-like conditions, mostly visible in the summer SSTs and seasonality records (Figure 4a).

[31] In core 1207, the sea surface conditions record a two-step change. By about 7.2 ka a first transition is recorded when lower summer SSTs are reached and SSSs shift to much higher values (~32 and ~33.5 in summer and winter, respectively). This regime ends at ~4.9 ka, corresponding with the second major change in assemblages. After ~4.9 ka, SSSs increase significantly and remain stable. Short-term variations are more weakly expressed in this record than in the one north of Iceland, and changes in the dinocyst assemblages mainly reflect the sea ice extent record (Figure 4b).

5. Discussion

5.1. Long-Term Trends of Holocene Climate in the Northwest Atlantic

[32] Sea surface reconstructions on the eastern Greenland and northern Iceland shelves depict coherent long-term Holocene trends. From the early to the late Holocene, February SSTs increase slightly, while August SSTs are more stable, except for a warm interval lasting from 10 to 8 ka in core 1207. As a result, seasonality decreases throughout the Holocene (Figure 4). SSS reconstructions, in winter as well as in summer, yield generally lower values in the early to mid-Holocene, a period that is also characterized by a more extensive sea ice cover. This situation is consistent with more pronounced low-salinity water supplies from the Arctic, which favor a stronger stratification through the formation of a buoyant and relatively fresh surface water layer. This strong stratification, by preventing the diffusion of heat from the atmosphere through the water column, results in a reduced thermal inertia in a surface layer that may have been relatively shallow. The surface water response to air temperatures is thus faster; summer warming up and winter cooling are more pronounced and seasonal contrast increases. This mechanism was probably reinforced in the early Holocene by a higher summer insolation and a weaker winter insolation [*Berger and Loutre*, 1991], as well as by additional freshwater supplies at the Greenland site due to the waning of the Greenland ice sheet, which lasted until ~8 ka [*Funder*, 1989]. Such a scenario is likely to explain the diatom-based summer SST reconstructions given by *Andersen et al.* [2004], which point to 2 to 4°C warmer early Holocene SSTs off eastern Greenland and northern Iceland compared to the mid-Holocene to late Holocene period. In the mid-Holocene to late Holocene, higher SSSs and shorter sea ice extent reflect an overall diminishing influence of polar waters and enhanced advection of Atlantic-source waters to the Denmark Strait region (Figure 4). The resulting weaker stratification leads to enhanced mixing and better diffusion of heat in the water column; seasonal changes of temperature are thus damped, which might explain the increasing winter SSTs and decreasing seasonality.

[33] This long-term trend of sea surface conditions is only partly consistent with previous studies in the same region, some of which yield a cooling summer trend in the late Holocene [e.g., *Andersen et al.*, 2004]. However, as said earlier, comparison with *Jiang et al.*'s [2002] diatom-based reconstructions shows a good overall coherency with our data. In addition, some indications of a long-term warming for the last 10 000 yrs, at least in winter or on an annual basis, can be inferred from the slightly diminishing relative abundance of cold planktonic foraminifera *Neogloboquadrina pachyderma* sinistral in a core from the Denmark Strait (VM28-14 [*Bond et al.*, 1997]), and to some extent from increased bulk carbonate accumulation in the mid-Holocene to late Holocene off northern Iceland [e.g.,

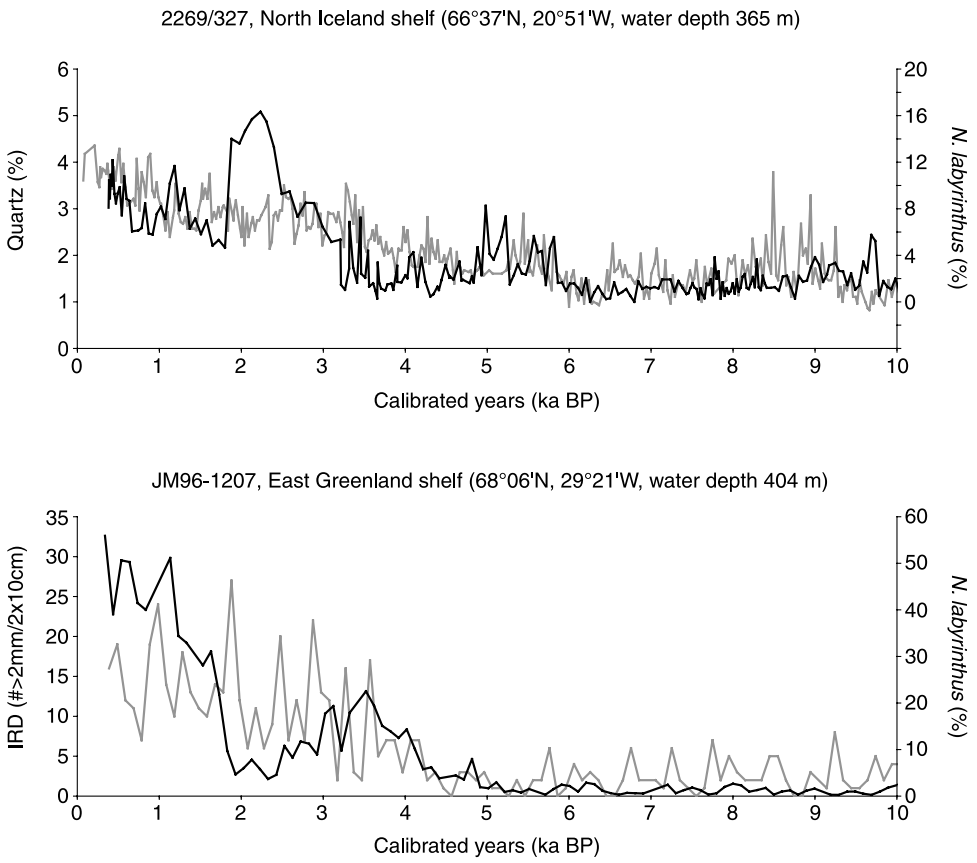

Figure 6. Comparison of the relative percentages of *N. labyrinthus* (black curves) with the IRD (core 1207 [*Jennings et al.*, 2002]) and quartz (core 2269 [*Moros et al.*, 2006]) records (gray curves).

Andrews and Giraudeau, 2003], a measure of productivity induced by nutrient-rich Atlantic waters. Warmer winter SSTs in the late Holocene are suggested by *Moros et al.* [2004b] as well.

[34] The inferred weakening of polar waters supplies on the eastern Greenland shelf and off northern Iceland seems at odd with the ice-rafted detritus (IRD) records in core 1207 [*Jennings et al.*, 2002] and on the east Greenland margin in general [*Andrews et al.*, 1997], as well as the quartz percentages record in core 2269 [*Moros et al.*, 2006], which are commonly interpreted as evidences for a late Holocene cooling trend and strengthened EGC and EIC circulation in the Denmark Strait region. A possible explanation for such a discrepancy could be related to Greenland outlet glacier ablation mechanisms. *Reeh et al.* [1999] and *Reeh* [2004] showed that glacier ablation is controlled by two different mechanisms, depending on the presence or absence of fast ice, which is in turn related to winter cold and summer warmth. A temperature increase of only a few degrees would be enough to switch from a floating glacier regime to an iceberg-calving glacier regime. While the former is associated with little IRD deposition on the shelf, the latter has a higher potential for transporting IRD out of the fjords [*Reeh et al.*, 1999; *Reeh*, 2004].

[35] A second explanation, sustained by our sea ice and temperature reconstructions might lay in the influence of sea ice upon the drifting of lithic grains-bearing icebergs calved from the Greenland ice sheet. As proposed by *Funder et al.* [1998] from observations in the Arctic areas and along east Greenland, and discussed by *Moros et al.* [2004a], IRD production is maximum in periods when there is both seasonally open water (low sea ice extent) and glacier fronts in an advanced position. The middle to late Holocene steady increase in IRD recorded in cores 1207 [*Jennings et al.*, 2002] and 2269 [*Moros et al.*, 2006] might therefore be viewed as primarily related to (1) lower sea ice concentrations in the Denmark Strait region due to enhanced influence of Atlantic waters and increased winter SSTs as indicated by our reconstructions, (2) the Neoglacial readvance of the Greenland ice sheet [*Fulton*, 1989; *Cuffey and Clow*, 1997] and nearby mountain glaciers in north Iceland [*Stötter et al.*, 1999]. Comparison of IRD/quartz records with the relative abundance of the dinocyst species *N. labyrinthus* shows a close correspondence between the two proxies (Figure 6). Nowadays, highest occurrences of *N. labyrinthus* are found off western Iceland, in the path of the IC, as well as in the Labrador Sea under the Atlantic-influenced WGC, whereas it is absent from regions with quasi-permanent sea ice cover such as the northeastern Greenland shelf [*Rochon et al.*, 1999]. The coherency between the *N. labyrinthus* and IRD/quartz records illustrate the key influence of Atlantic water inflow upon the delivery of ice-rafted lithic material to the Denmark Strait region. Hence we propose that the increased IRD content in late Holocene sediments off eastern Greenland and northern Iceland, is an indication of a fundamental shift in delivery of IRD to the Denmark Strait region. This shift was

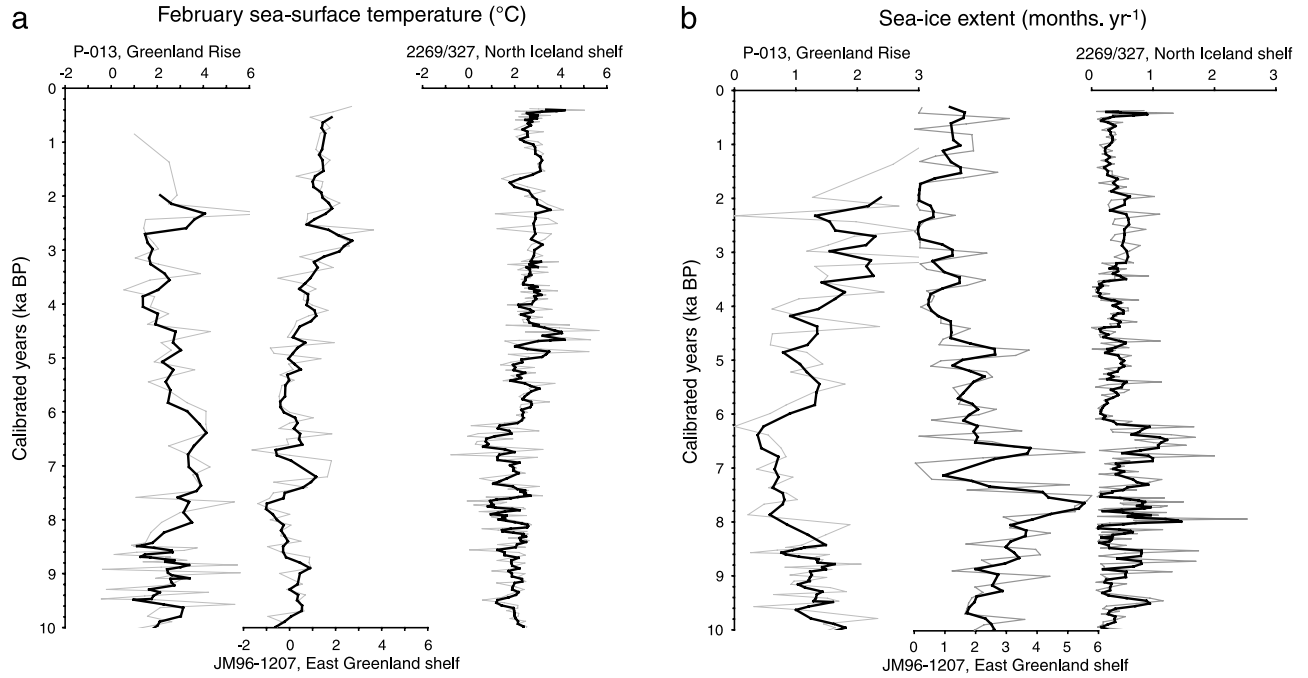

Figure 7. Comparison of some of the reconstructed parameters from cores 2269/327 and 1207 with those from core P-013, Greenland Rise [*Solignac et al.*, 2004]. Note the different horizontal scales. Bold curves are smoothed records (three-point running mean). Reconstructions for record P-013 were updated with the latest "n = 940" dinocyst database [*de Vernal et al.*, 2005] and the updated World Ocean Atlas [*NODC*, 2001].

triggered by the coupled dynamics of continental ice sheet, and surface circulation changes linked to warmer winter SSTs and associated decreasing sea ice extent.

5.2. Spatial Heterogeneity in Surface Water Conditions Across the NW Atlantic

[36] The long-term coherent pattern of sea surface condition changes recorded off eastern Greenland and northern Iceland must be viewed as the response of the Iceland and Greenland seas to the progressively reduced influence of polar waters relative to the Atlantic waters in the western Nordic seas. This regional coherency is further amplified by the EIC, which effectively connects both shelf settings. However, much damper long-term trends on the north Iceland shelf as well as several short-term discrepancies between the two records point out the role of distinct local surface circulation features that may respond differently or in a delayed manner to a combination of climate forcings.

[37] Discrepancies are particularly pronounced on a shorter millennial to centennial timescale. Moreover, the discrepancies also concern the timing of the main changes: most records from the northern Iceland shelf present a clear shift around 6.2 ka, whereas a strong regime change associated with a drop in summer SSTs and a dramatic increase in SSSs occurs at ~7.4 ka off Greenland. A second major change in core 1207 takes place at ~4.9 ka, this time apparent only in the SSS (increase) and sea ice extent (decrease) records (Figure 4b). A possible explanation for these discrepancies between the two sites could be linked to the proximity of site 1207 to the Greenland ice sheet. We can hypothesize that site 1207, which lies close to the east Greenland coast on the inner shelf, was more directly affected by meltwater coming from the Greenland ice sheet in the early and mid-Holocene. In contrast, the northern Iceland site does not seem to have been as much influenced by meltwater supplies, as SSSs as low as those measured off eastern Greenland do not appear in our record.

[38] The spatial and temporal heterogeneity in the northwestern Atlantic is further illustrated when comparing hydrological changes in our records with those from site P-013, located south of Greenland (Figure 1; see also *de Vernal and Hillaire-Marcel* [2000] and *Solignac et al.* [2004] for further details). Site P-013, in the northeastern Labrador Sea, is under the influence of the West Greenland Current (WGC), which carries a mix of cold polar water from the ECG and warm salty water from the western branch of the IC (Figure 1).

[39] Records from east and south Greenland depict anticorrelated long-term trends that are especially clear in the winter SSTs and sea ice extent signals of the mid-Holocene and late Holocene (Figure 7). These discrepancies between the records imply that waters from the Arctic that reached the eastern Greenland were not carried all the way to the southern Greenland site. The observed long-term corresponding trends from the eastern Greenland and northern Iceland shelves additionally suggest that an important part of this meridional flow of polar waters was deflected toward the east via the EIC.

[40] The IC component of the WGC probably played an important role as well in determining sea surface conditions south of Greenland. The thermal optimum from ~8.0 to 5.5 ka in core P-013 could be related to an enhanced western

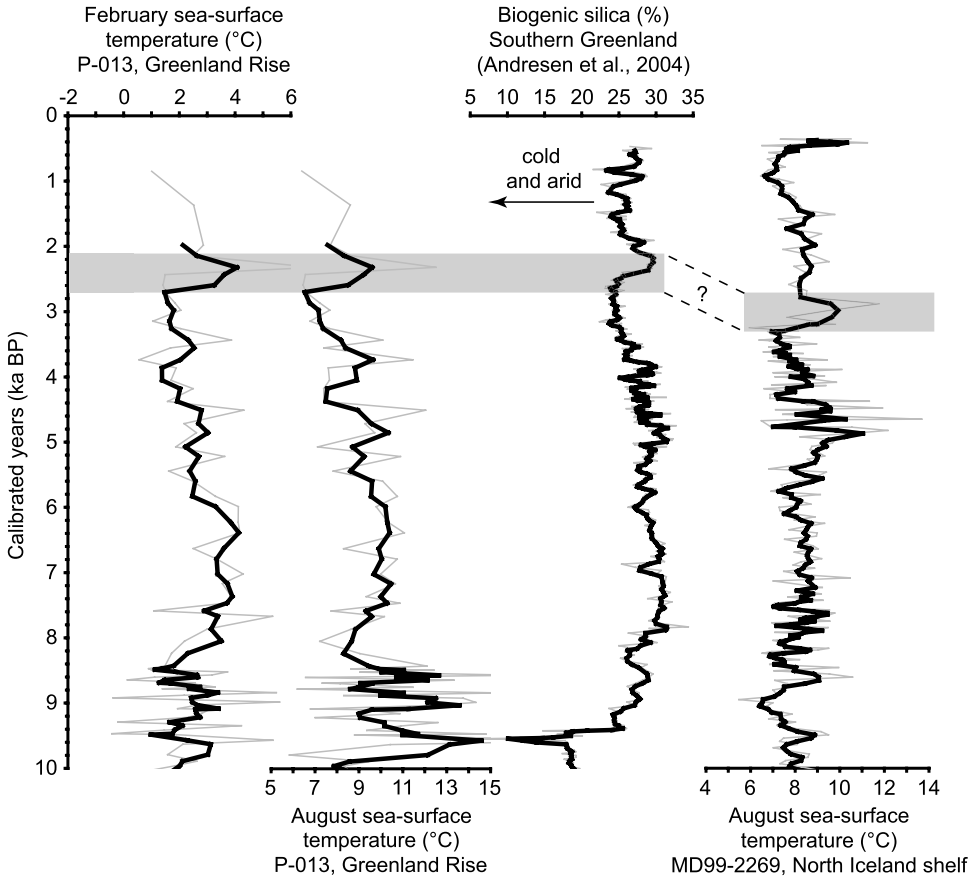

Figure 8. Comparison of dinocyst-based reconstructions of SSS and SST from cores P-013 and 2269/327 with a continental biogenic silica record from Lake N14, southern Greenland [*Andresen et al.*, 2004].

branch of the IC carrying more intensively warm waters to the south of Greenland. After 5.5 ka, the influence of the IC in the northeastern Labrador Sea apparently decreased, resulting in colder SSTs and more extensive sea ice cover.

[41] Despite the theoretical surface circulation connection between southern Greenland and northern Iceland via both branches of the IC (Figure 1), we see an overall anticorrelation of the reconstructed winter sea surface temperature and sea ice extent records between both core sites (P-013 and 2269/327) (Figures 4a and 7). Part of this inconsistency may lay in the fact that the 2269/327 record, being influenced by both the EIC and the NIIC, delivers a mixed signal, in which the variations of the two currents occult one another. Another explanation, sustained by the record of dinocyst assemblages from 2269/327, could be a balance between the two branches of this surface current throughout the Holocene, the western branch feeding the southern Greenland and Labrador Sea areas being strengthened (reduced) during period of reduced (strengthened) flow of Irminger water around Iceland.

[42] Coherence is clearly shown between the record of core P-013 and a continental record from Lake N14 in southern Greenland (Figures 1 and 8). In the latter record, *Andresen et al.* [2004] interpreted the relative contribution of biogenic silica as a proxy for atmospheric conditions over South Greenland, low values corresponding to low primary production in a cold and arid environment, whereas high values are associated to higher annual production related to warm and humid conditions. The biogenic silica record follows reconstructed SSTs of site P-013, although only after ~8.2 ka for the summer SSTs due to the strong influence of meltwaters until then [*Funder*, 1989] that form a floating freshwater surface layer. The coherence between the south Greenland lake and core P-013 data after 8.2 ka points to the determinant influence of the western branch of the IC in the southern Greenland area and Labrador Sea. Some correlations can be proposed as well with the August SSTs from core 2269/327, with the maximum reconstructed values at ~4.7 ka in core 2269/327 being recorded in biogenic silica as well (Figure 8). This coherence between the southern Greenland and north Iceland records suggests that this short interval was a time of equilibrium in the influence of the IC between its western and northern branches, at least in summer. The second 2269/327 SST maximum at ~2.7 ka could correlate with the warm event seen in both the February SSTs from core P-013 and the southern Greenland lake at ~2.4 ka, although not enough evidence is available at this stage to assert it. Uncertainties about the reservoir age on the northern Iceland shelf [*Eiriksson et al.*, 2000; *Haflidason et al.*, 2000] as well as a somewhat poorly constrained age model for core 327, emphasize the need for a more refined chronostratigraphy to

further assess the coherence between the northern Iceland shelf and southern Greenland.

5.3. Atmospheric Forcing in the NW Atlantic

[43] Temperatures and precipitations in southern Greenland are presently related to the location of the low-pressure system along its track, which crosses this area from south of Greenland to the northeast. When the position of the Icelandic Low is closer to southern Greenland, easterly winds bring warm temperatures and increased precipitation. Inversely, a northeastern position near Iceland implies northwesterly winds that bring cold and arid weather over southern Greenland [*Andresen et al.*, 2004].

[44] The connection between the continental record from South Greenland and the P-013 record in the path of the western branch of the IC suggests a coupling between the atmospheric processes described above and the dynamics of the IC. We hypothesize that a southwesterly position of the Icelandic Low that seems to prevail in the early to mid-Holocene (~9 to 5.5 ka) and associated easterly/southeasterly winds are responsible for a strengthening of the influence of Atlantic waters to the south of Greenland through the IC, thus increasing SSTs and SSSs and decreasing sea ice extent in core P-013. After 5.5 ka, overall lower biogenic silica percentages in the South Greenland Lake N14 indicate generally colder and more arid climate in southern continental Greenland [*Andresen et al.* [2004] (Figure 8). The position of the Icelandic Low must thus have shifted to the northeast throughout the Holocene. We surmise that such a shift favored the rerouting of Atlantic waters toward western Iceland and eastern Greenland to the prejudice of the southern Greenland region. Accordingly, at 5.5 ka, SSTs in core P-013 south of Greenland decrease, suggesting a weakening of the influence of the western branch of the IC. On the eastern Greenland and north Iceland shelves, SSSs increase and stabilize, and winter SSTs increase steadily, indicating reduced water advection from the Arctic and enhanced flow of Atlantic waters through the northern branch of the IC. This scenario is mostly sustained by winter SST reconstructions and sea ice extent.

[45] The shift of the Iceland Low throughout the Holocene bears some resemblance with the dominant mode of present winter climate variability in the North Atlantic region, that is, the North Atlantic Oscillation (NAO) [*Hurrell*, 1995]. The antiphase relationship documented in the present work between winter conditions in the southern Greenland region and the Denmark Strait area might be viewed as related to long-term changes in the phase of the NAO, with a progressive shift from a negative phase in the Early Holocene to a positive phase from the mid-Holocene onward. Lower (higher) sea ice concentration and higher (lower) SSTs south of Greenland, combined with higher (lower) sea ice extent and fresher (saltier) and colder (warmer) sea surface conditions in the Greenland Sea region are indeed a signature of a negative (positive) NAO phase [*Chapman and Walsh*, 1993; *Visbeck et al.*, 2003]. Our observations are coherent with the work of *Tremblay et al.* [1997] on driftwood records in the Arctic Ocean, in which a strong EGC associated with a negative phase of the NAO and a southerly position of the Icelandic Low characterize the early Holocene, followed by a weak EGC linked to a positive phase of the NAO in the mid-Holocene to late Holocene. However, such a long-term change in the phase of the NAO does not win unanimous support among the different studies; other reconstructions, based, for example, on alkenone data [*Rimbu et al.*, 2003] or diatom assemblages [*Andersen et al.*, 2004] suggest an opposite evolution of this atmospheric circulation pattern. It must be kept in mind as well that local atmospheric forcings other than the NAO might play a determinant role in climate and sea surface variability in the western North Atlantic. Notably, instrumental records do not seem to show any connection between the NAO index and the Atlantic inflow off western and northern Iceland [*Ólafsson*, 1999]. We therefore surmise that any assumption of NAO-forced evolution of the sea surface conditions throughout the Holocene in the Nordic seas should take into account additional local processes.

6. Conclusions

[46] Comparison of Holocene sea surface conditions at three different environments of the North Atlantic, each under the influence of a different combination of currents but nevertheless in interaction with each other, depicts a strong spatial heterogeneity.

[47] Site 1207 on the east Greenland shelf, characterized by polar waters carried by the EGC, shows warming winter SSTs and diminishing sea ice extent trends throughout the Holocene. The same is observed at site 2269/327 on the north Iceland shelf, which lies in the path of the warm NIIC and the Arctic EIC, while site P-013 south of Greenland, influenced by the EGC and the IC, depicts opposite trends. This suggests that increased polar water supplies on the east Greenland shelf during the early to mid-Holocene were mostly deflected toward the northern Iceland shelf and did not efficiently reach the south of Greenland where conditions are indicative of a sustained Atlantic water influence. A decoupled dynamics of the western branch of the IC and of the NIIC could be the cause of such a discrepancy.

[48] Our surface water reconstructions are at first glance at odd with the commonly assumed late Holocene cooling of the Denmark Strait region as previously suggested by IRD records. On the basis of the dinocyst-based reconstruction of sea ice extent off eastern Greenland and northern Iceland, as well as of the close relationship between the abundances of an Atlantic dinocyst species, *Nematosphaeropsis labyrinthus*, and IRD contents in the studied cores, we believe that IRD delivery in the Denmark Strait region during the Holocene is favored by a combination of sustained iceberg calving from the Greenland ice sheet, as well as reduced sea ice cover to allow the transfer of lithic materials from its source to distant areas such as the north Iceland shelf. Consequently, the late Holocene increase in IRD sedimentation across this region might be viewed as triggered by an increased Atlantic water inflow (and associated lower sea ice extent), and the Neoglacial readvance of the Greenland ice sheet after its early Holocene decay.

[49] The coherence between core P-013 on the southern Greenland rise and a continental record in southern Greenland puts forward a close coupling between the atmosphere and the

ocean, with a general pattern of the Icelandic Low shifting northeastward throughout the Holocene. Combined with a weakening EGC throughout the Holocene, this atmospheric evolution is reminiscent of a long-term evolution of the NAO (from a negative phase in the early Holocene to a positive phase onward). Any firm assumption of a NAO-forced Holocene history of the hydrography of the NW Atlantic, however, needs additional work, and must consider the evolution of additional local atmospheric forcing such as those presently acting in the Denmark Strait and nearby regions.

[50] **Acknowledgments.** We are indebted to Anne Jennings and John T. Andrews, INSTAAR, Boulder, Colorado, for access to the samples, as well as to C. Andresen (GeoBiosphere Science Centre, Lund, Sweden), A. Jennings, H. Jiang (East China Normal University, Shanghai), and M. Moros (Bjerknes Centre for Climate Research, Bergen, Norway) for sharing their data. Fruitful discussions with M. Moros and J.-L. Turon (EPOC, Université Bordeaux 1, Talence, France), as well as comments from an anonymous reviewer and J. Matthiessen (Alfred Wegener Institute, Bremerhaven, Germany) helped improve this paper. Core MD99-2269 was collected as part of IMAGES V, Leg 3 cruise of the R/V *Marion Dufresne*, under the leadership of J.-L. Turon (chief scientist) and Y. Balut (IPEV, chief of operations), and support from IPEV and CNRS/INSU. This study is a contribution to project GR-240 of the Canadian Foundation for Climate and Atmospheric Sciences and to the project TARDHOL of the French Programme National d'Études de la Dynamique du Climat of CNRS-INSU. Support was also provided by the Natural Sciences and Engineering Research Council of Canada. Special thanks are due to David Fortin (Environmental Extremes and Variability Laboratory, Department of Geography, Queen's University, Kingston, Canada) for helpful comments on this manuscript.

References

Alley, R. B., A. M. Agustsdottir, and P. J. Fawcett (1999), Ice-core evidence of late-Holocene reduction in North Atlantic Ocean heat transport, in *Mechanisms of Global Climate Change at Millennial Time Scales*, *Geophys. Monogr. Ser.*, vol. 112, edited by P. U. Clark, R. S. Webb, and L. D. Keigwin, pp. 301–312, Washington, D. C.

Andersen, C., N. Koç, A. Jennings, and J. T. Andrews (2004), Nonuniform response of the major surface currents in the Nordic seas to insolation forcing: Implications for the Holocene climate variability, *Paleoceanography*, *19*, PA2003, doi:10.1029/2002PA000873.

Andresen, C. S., S. Björck, O. Bennike, and G. Bond (2004), Holocene climate changes in southern Greenland: Evidence from lake sediments, *J. Quat. Sci.*, *19*, 783–795.

Andresen, C. S., G. Bond, A. Kuijpers, P. C. Knutz, and S. Björck (2005), Holocene climate variability at multidecadal time scales detected by sedimentological indicators in a shelf core NW off Iceland, *Mar. Geol.*, *214*, 323–338.

Andrews, J. T., and J. Giraudeau (2003), Multi-proxy records showing significant Holocene environmental variability: The inner N. Iceland shelf (Hunafloi), *Quat. Sci. Rev.*, *22*, 175–193.

Andrews, J. T., L. M. Smith, R. Preston, T. Cooper, and A. Jennings (1997), Spatial and temporal patterns of iceberg rafting (IRD) along the east Greenland margin, ca. 68°N, over the last 14 cal. ka, *J. Quat. Sci.*, *12*, 1–13.

Andrews, J. T., G. Helgadóttir, A. Geirsdóttir, and A. E. Jennings (2001a), Multicentury-scale records of carbonate (hydrographic?) variability on the N Iceland margin over the last 5000 yrs, *Quat. Res.*, *56*, 199–206.

Andrews, J. T., G. B. Kristjánsdóttir, A. Geirsdóttir, J. Hardardóttir, G. Helgadóttir, A. E. Sveinbjörnsdóttir, A. E. Jennings, and L. M. Smith (2001b), Late Holocene (~5 cal ka) trends and century-scale variability of N. Iceland marine records: Measures of surface hydrography, productivity, and land/ocean interactions, in *The Oceans and Rapid Climate Change: Past, Present, and Future*, *Geogphys. Monogr. Ser.*, vol. 126, edited by D. Seidov, B. J. Haupt, and M. Maslin, pp. 69–81, AGU, Washington, D. C.

Andrews, J. T., R. Kihl, G. B. Kristjánsdóttir, L. M. Smith, G. Helgadóttir, A. Geirsdóttir, and A. E. Jennings (2002), Holocene sediment properties of the east Greenland and Iceland continental shelves bordering Denmark Strait (64–68°N), North Atlantic, *Sedimentology*, *49*, 5–24.

Andrews, J. T., J. Hardardóttir, G. B. Kristjansdóttir, K. Grönvold, and J. S. Stoner (2003), A high-resolution Holocene sediment record from Hunuaflóaáll, N Iceland margin: Century- to millennial-scale variability since the Vedde tephra, *Holocene*, *13*, 625–638.

Belkin, I. M., S. Levitus, J. Antonov, and S.-A. Malmberg (1998), "Great salinity anomalies" in the North Atlantic, *Prog. Oceanogr.*, *41*, 1–68.

Berger, A. L., and M. F. Loutre (1991), Insolation values for the climate of the last 10 million years, *Quat. Sci. Rev.*, *10*, 297–317.

Bianchi, G. G., and I. N. McCave (1999), Holocene periodicity in North Atlantic climate and deep-ocean flow south of Iceland, *Nature*, *397*, 515–517.

Boessenkool, K. P., M.-J. van Gelder, H. Brinkhuis, and S. R. Troelstra (2001), Distribution of organic-walled dinoflagellate cysts in surface sediments from transects across the polar front offshore southeast Greenland, *J. Quat. Sci.*, *16*, 661–666.

Bond, G., W. Showers, M. Cheseby, R. Lotti, P. Almasi, P. de Menocal, P. Priore, H. Cullen, I. Hajdas, and G. Bonani (1997), A pervasive millennial-scale cycle in North Atlantic Holocene and glacial climates, *Science*, *278*, 1257–1266.

Campbell, I. D., C. Campbell, M. J. Apps, N. W. Rutter, and A. B. G. Bush (1998), Late Holocene ~1500 yr climatic periodicities and their implications, *Geology*, *26*, 471–473.

Castañeda, I., M. Smith, G. B. Kristjánsdóttir, and J. T. Andrews (2004), Temporal changes in Holocene $\delta^{18}O$ records from the northwest and central north Iceland shelf, *J. Quat. Sci.*, *19*, 321–334.

Chapman, W. L., and J. E. Walsh (1993), Recent variations of sea ice and air temperature in high latitudes, *Bull. Am. Meteorol. Soc.*, *74*, 33–47.

Cuffey, K. M., and G. D. Clow (1997), Temperature, accumulation, and ice sheet elevation in central Greenland through the last glacial transition, *J. Geophys. Res.*, *102*, 26,383–26,396.

de Vernal, A., and C. Hillaire-Marcel (2000), Sea-ice cover, sea-surface salinity and halo-/thermocline structure of the northwest North Atlantic: Modern versus full glacial conditions, *Quat. Sci. Rev.*, *19*, 65–85.

de Vernal, A., J.-L. Turon, and J. Guiot (1994), Dinoflagellate cyst distribution in high-latitude marine environments and quantitative reconstruction of sea-surface salinity, temperature and seasonality, *Can. J. Earth Sci.*, *31*, 48–62.

de Vernal, A., M. Henry, and G. Bilodeau (1999), Technique de préparation et d'analyse en micropaléontologie, *Cah. GEOTOP*, *3*, report, Univ. du Quebec à Montreal, Montreal, Canada.

de Vernal, A., et al. (2001), Dinoflagellate cyst assemblages as tracers of sea-surface conditions in the northern North Atlantic, Arctic and sub-Arctic seas: The new "n = 677" database and application for quantitative paleoceanographical reconstruction, *J. Quat. Sci.*, *16*, 681–699.

de Vernal, A., et al. (2005), Reconstruction of sea-surface conditions at middle to high latitudes of the Northern Hemisphere during the Last Glacial Maximum (LGM) based on dinoflagellate cyst assemblages, *Quat. Sci. Rev.*, *24*, 897–924.

Eiriksson, J., K. L. Knudsen, H. Haflidason, and J. Heinemeier (2000), Chronology of late Holocene climatic events in the northern North Atlantic based on AMS ^{14}C dates and tephra markers from the volcano Hekla, Iceland, *J. Quat. Sci.*, *15*, 573–580.

Fulton, R. J. (Ed.) (1989), *Quaternary Geology of Canada and Greenland*, *Geol. Can.*, vol. 1, pp. 1–11, Geol. Surv. Of Can., Ottawa.

Funder, S. (1989), Quaternary geology of ice-free areas and adjacent shelves of Greenland, in *Quaternary Geology of Canada and Greenland*, *Geol. Can.*, vol. 1, edited by R. J. Fulton, pp. 743–792, Geol. Surv. Of Can., Ottawa.

Funder, S., C. Hjort, J. Y. Landvik, S.-I. Nam, N. Reeh, and R. Stein (1998), History of a stable ice margin—East Greenland during the middle and upper Pleistocene, *Quat. Sci. Rev.*, *17*, 77–123.

Giraudeau, J., A. E. Jennings, and J. T. Andrews (2004), Timing and mechanisms of surface and intermediate water circulation changes in the Nordic seas over the last 10,000 cal years: A view from the north Iceland shelf, *Quat. Sci. Rev.*, *23*, 2127–2139.

Guiot, J., and C. Goeury (1996), PPPbase, a software for statistical analysis of paleoecological data, *Dendrochronologia*, *14*, 295–300.

Haflidason, H., J. Eiriksson, and S. van Kreveld (2000), The tephrochronology of Iceland and the North Atlantic region during the middle and late Quaternary: A review, *J. Quat. Sci.*, *15*, 3–22.

Head, M. J., R. Harland, and J. Matthiessen (2001), Cold marine indicators of the late Quaternary: The new dinoflagellate cyst genus *Islandinium* and related morphotypes, *J. Quat. Sci.*, *16*, 621–636.

Helgadóttir, G. (1997), Paleoclimate (0 to >14 ka) of W and NW Iceland: An Iceland/USA contribution to P.A.L.E, *Cruise Rep. B9-97*, Mar. Res. Inst. of Iceland, Reykjavik.

Hjort, C. (1973), A sea correction for east Greenland, *Geol. Foeren. Stockholm Foerh.*, *95*, 132–134.

Hopkins, T. S. (1991), The GIN Sea: A synthesis of its physical oceanography and literature review 1972–1985, *Earth Sci. Rev.*, *30*, 175–318.

Hurrell, J. W. (1995), Decadal trends in the North Atlantic Oscillation: Regional temperatures and precipitation, *Science*, *269*, 376–379.

Isemer, H.-J., , and L. Hasse (Eds.) (1985), *The Bunker Climate Atlas of the North Atlantic Ocean*, vol. 1, *Observations*, pp. 57–60, Springer, New York.

Jennings, A. E., K. L. Knudsen, M. Hald, C. V. Hansen, and J. T. Andrews (2002), A mid-Holocene shift in Arctic sea-ice variability on the east Greenland shelf, *Holocene*, *12*, 49–58.

Jiang, H., M. S. Seidenkrantz, K. L. Knudsen, and J. Eiriksson (2001), Diatom surface sediment assemblages around Iceland and their relationships to oceanic environmental variables, *Mar. Micropaleontol.*, *41*, 73–96.

Jiang, H., M. S. Seidenkrantz, K. L. Knudsen, and J. Eiriksson (2002), Late-Holocene summer sea-surface temperatures based on a diatom record from the north Icelandic shelf, *Holocene*, *12*, 137–147.

Johannessen, O. M. (1986), Brief overview of the physical oceanography, in *The Nordic Seas*, edited by B. G. Hurdle, pp. 103–127, Springer, New York.

Knudsen, K. L., J. Eiriksson, E. Jansen, H. Jiang, F. Rytter, and E. R. Gudmundsdottir (2004), Paleoceanographic changes off North Iceland through the last 1200 years: Foraminifera, stable isotopes, diatoms, and ice rafted debris, *Quat. Sci. Rev.*, *23*, 2231–2246.

Malmberg, S.-A. (1985), The water masses between Iceland and Greenland, *J. Mar. Res. Inst.*, *9*, 127–140.

Malmberg, S.-A., and S. Jónsson (1997), Timing of deep convection in the Greenland and Iceland seas, *ICES J. Mar. Sci.*, *54*, 300–309.

Marchal, O., et al. (2002), Apparent cooling of the sea surface in the northeast Atlantic and Mediterranean during the Holocene, *Quat. Sci. Rev.*, *21*, 455–483.

Marret, F., J. Eiríksson, K. L. Knudsen, J.-L. Turon, and J. D. Scourse (2004), Distribution of dinoflagellate cyst assemblages in surface sediments from the northern and western shelf of Iceland, *Rev. Paleobot. Palynol.*, *128*, 35–53.

Matthews, J. (1969), The assessment of a method for the determination of absolute pollen frequencies, *New Phytol.*, *68*, 161–166.

Matthiessen, J. (1995), Distribution patterns of dinoflagellate cysts and other organic-walled microfossils in recent Norwegian-Greenland Sea sediments, *Mar. Micropaleontol.*, *24*, 307–334.

Matthiessen, J., et al. (2001), Distribution of calcareous, siliceous and organic-walled planktic microfossils in surface sediments of the Nordic seas and their relation to surface-water masses, in *The Northern North Atlantic: A Changing Environment*, edited by P. Schäfer et al., pp. 105–127, Springer, New York.

Matthiessen, J., A. de Vernal, M. Head, Y. Okolodkov, K. Zonneveld, and R. Harland (2005), Modern organic-walled dinoflagellate cysts in Arctic marine environments and their (paleo-) environmental significance, *Palaeontol. Z.*, *79*(1), 3–51.

Moros, M., J. F. McManus, T. Rasmussen, A. Kuijpers, T. Dokken, I. Snowball, T. Nielsen, and E. Jansen (2004a), Quartz content and the quartz-to-plagioclase ratio determined by X-ray diffraction: A proxy for ice rafting in the northern North Atlantic?, *Earth Planet. Sci. Lett.*, *218*, 389–401.

Moros, M., K. Emeis, B. Risebrobakken, I. Snowball, A. Kuijpers, J. McManus, and E. Jansen (2004b), Sea surface temperatures and ice rafting in the Holocene North Atlantic: Climate influences on northern Europe and Greenland, *Quat. Sci. Rev.*, *23*, 2113–2126.

Moros, M., J. T. Andrews, D. E. Eberl, and E. Jansen (2006), Holocene history of drift ice in the northern North Atlantic: Evidence for different spatial and temporal modes, *Paleoceanography*, doi:10.1029/2005PA001214, in press.

Mudie, P. J., and A. Rochon (2001), Distribution of dinoflagellate cysts in the Canadian Arctic marine region, *J. Quat. Sci.*, *16*, 603–620.

Naval Oceanography Command Detachment (1986), *Sea Ice Climatic Atlas: Vol. II, Arctic East*, *NAVAIR 50-1c-541*, 147 pp., Asheville, N. C.

National Oceanographic Data Center (NODC) (2001), World ocean atlas, http://www.nodc.noaa.gov/OC5/WOD01/pr_wod01.html, Silver Spring, Md.

National Snow and Ice Data Center (NSIDC) (2003), Arctic and Southern Ocean sea ice concentrations, http://nsidc.org/data/docs/noaa/g00799_arctic_southern_sea_ice/index.html, Boulder, Colo.

O'Brien, S. R., P. A. Mayewski, L. D. Meeker, D. A. Meese, M. S. Twickler, and S. I. Whitlow (1995), Complexity of Holocene climate as reconstructed from a Greenland ice core, *Science*, *270*, 1962–1964.

Ólafsson, J. (1999), Connection between oceanic conditions off N-Iceland, Lake Mývatn temperature, regional wind direction variability and the North Atlantic Oscillation, *Rit Fiskideildar*, *16*, 41–57.

Reeh, N. (2004), Holocene climate and fjord glaciations in northeast Greenland: Implications for IRD deposition in the North Atlantic, *Sediment. Geol.*, *165*, 333–342.

Reeh, N., C. Mayer, H. Miller, H. H. Thomsen, and A. Weidick (1999), Present and past climate control on fjord glaciations in Greenland: Implications for IRD-deposition in the sea, *Geophys. Res. Lett.*, *26*, 1039–1042.

Rimbu, N., G. Lohmann, J.-H. Kim, H. W. Arz, and R. Schneider (2003), Arctic/North Atlantic Oscillation signature in Holocene sea surface temperature trends as obtained from alkenone data, *Geophys. Res. Lett.*, *30*(6), 1280, doi:10.1029/2002GL016570.

Rochon, A., A. de Vernal, J.-L. Turon, J. Matthiessen, and M. J. Head (1999), *Distribution of Recent Dinoflagellate Cysts in Surface Sediments From the North Atlantic Ocean and Adjacent Seas in Relation to Sea-Surface Parameters*, *Contrib. Ser.*, vol. 35, pp. 7–54, Am. Assoc. of Stratigr. Palynol., Houston, Tex.

Solignac, S., A. de Vernal, and C. Hillaire-Marcel (2004), Holocene sea-surface conditions in the North Atlantic—Contrasted trends and regimes in the western and eastern sectors (Labrador Sea vs. Iceland Basin), *Quat. Sci. Rev.*, *23*, 319–334.

Steig, E. (1999), Mid-Holocene climate change, *Science*, *286*, 1485–1487.

Stötter, J., M. Wastl, C. Caseldine, and T. Haberle (1999), Holocene paleoclimatic reconstructions in Northern Iceland: Approaches and results, *Quat. Sci. Rev.*, *18*, 457–474.

Tremblay, L. B., L. A. Mysak, and A. S. Dyke (1997), Evidence from driftwood records for century-to-millennial scale variations of the high latitude atmospheric circulation during the Holocene, *Geophys. Res. Lett.*, *24*, 2027–2030.

Visbeck, M., E. P. Chassignet, R. G. Curry, T. L. Delworth, R. R. Dickson, and G. Krahmann (2003), The ocean's response to North Atlantic Oscillation variability, in *The North Atlantic Oscillation: Climate Significance and Environmental Impact*, *Geophys. Monogr. Ser.*, vol. 134, edited by J. W. Hurrell et al., pp. 113–145, AGU, Washington, D. C.

A. de Vernal and S. Solignac, GEOTOP, Université du Québec à Montréal, Case postale 8888, Succursale Centre-Ville, Montréal, QC, Canada H3C 3P8. (devernal.anne@uqam.ca; solignac.sandrine@courrier.uqam.ca)

J. Giraudeau, Environnements et Paléoenvironnements Océaniques, UMR CNRS 5805, Université Bordeaux 1, Avenue des Facultés, F-33405 Talence cedex, France. (j.giraudeau@epoc.u-bordeaux1.fr)